Biochemical and Biophysical Research Communications 407 (2011) 148–152

Contents lists available at ScienceDirect

Biochemical and Biophysical Research Communications

journal homepage: www.elsevier.com/locate/ybbrc

The effect of transcutaneous application of carbon dioxide (CO_2) on skeletal muscle

Keisuke Oe [a,1], Takeshi Ueha [b,1], Yoshitada Sakai [c,*], Takahiro Niikura [a], Sang Yang Lee [a], Akihiro Koh [a], Takumi Hasegawa [d], Masaya Tanaka [b], Masahiko Miwa [a], Masahiro Kurosaka [a]

[a] Department of Orthopaedic Surgery, Kobe University Graduate School of Medicine, Kobe, Japan
[b] NeoChemir Inc, Kobe, Japan
[c] Faculty of Health Care Sciences, Himeji Dokkyo University, Himeji, Japan
[d] Department of Oral and Maxillofacial Surgery, Kobe University Graduate School of Medicine, Kobe, Japan

ARTICLE INFO

Article history:
Received 24 February 2011
Available online 1 March 2011

Keywords:
PGC-1α
Transcutaneous application of carbon dioxide
Muscle fiber changing
Mitochondrial biogenesis

ABSTRACT

In Europe, carbon dioxide therapy has been used for cardiac disease and skin problems for a long time. However there have been few reports investigating the effects of carbon dioxide therapy on skeletal muscle. Peroxisome proliferators-activated receptor (PPAR)-gamma coactivator-1 (PGC-1α) is up-regulated as a result of exercise and mediates known responses to exercise, such as mitochondrial biogenesis and muscle fiber-type switching, and neovascularization via up-regulation of vascular endothelial growth factor (VEGF). It is also known that silent mating type information regulation 2 homologs 1 (SIRT1) enhances PGC-1α-mediated muscle fiber-type switching. Previously, we demonstrated transcutaneous application of CO_2 increased blood flow and a partial increase of O_2 pressure in the local tissue known as the Bohr effect. In this study, we transcutaneously applied CO_2 to the lower limbs of rats, and investigated the effect on the fast muscle, tibialis anterior (TA) muscle. The transcutaneous CO_2 application caused: (1) the gene expression of PGC-1α, silent mating type information regulation 2 homologs 1 (SIRT1) and VEGF, and increased the number of mitochondria, as proven by real-time PCR and immunohistochemistry, (2) muscle fiber switching in the TA muscle, as proven by isolation of myosin heavy chain and ATPase staining. Our results suggest the transcutaneous application of CO_2 may have therapeutic potential for muscular strength recovery resulting from disuse atrophy in post-operative patients and the elderly population.

1. Introduction

The benefits of the carbonated spa (carbon dioxide therapy) have long been known in Europe, and it is understood that carbon dioxide therapy is effective in treating cardiac diseases and skin problems [1–4]. An example is the use of artificial CO_2 enriched water bathing, which has been clinically applied to improve ischemic limb symptoms [2–4]. In plastic surgery, subcutaneous injection of CO_2 is applied if skin irregularity and/or adiposity occur [5,6]. These therapeutic effects of CO_2 are caused by an increase in blood flow and microcirculation, nitric oxide-dependent neocapillary formation, and a partial increase of O_2 pressure in the local tissue known as the Bohr effect [2,4,6]. Recently, we demonstrated that transcutaneous application of CO_2 up-regulated O_2 pressure in the local tissue using NIRS [7].

However, to date, there have been few reports investigating the effects of carbon dioxide therapy on skeletal muscle. We hypothesized that the transcutaneous application of CO_2 to muscle would promote a similar effect to aerobic exercise. In other words, the increase of O_2 pressure in local muscle caused by the transcutaneous application of CO_2 in the absence of proper exercise could induce a similar effect to aerobic exercise. Generally muscle fiber-type switching is caused by an up-regulating peroxisome proliferators-activated receptor (PPAR)-gamma coactivator-1 (PGC-1α) gene and a number of mitochondria. It is also known that silent mating type information regulation 2 homologs 1 (SIRT1) enhances PGC-1α-mediated muscle fiber-type switching. PGC-1α, the number of mitochondria, and SIRT1 are all up-regulated as a result of aerobic exercise [8].

In this study, we transcutaneously applied CO_2 to the lower limbs of rats, and investigated the effect on the fast muscle (tibialis anterior muscle; TA muscle) by analyzing the gene expression of PGC-1α, SIRT1, and vascular endothelial growth factor (VEGF), the number of mitochondria, and immunolocalization of PGC-1α, SIRT1, and VEGF, and muscle fiber-type switching.

2. Materials and methods

2.1. Experimental set up

The use of animals was approved by the Animal Care and Use Committee of Kobe University Graduate School of Medicine.

* Corresponding author. Address: Faculty of Health Care Sciences, Himeji Dokkyo University, 7-2-1, Kami-Ohno, Himeji, Hyogo 6708524, Japan. Fax: +81 79 223 6714.
E-mail address: sakai.yoshitada@gm.himeji-du.ac.jp (Y. Sakai).
[1] Dr. Oe and Mr. Ueha contributed equally to this work.

0006-291X/$ - see front matter © 2011 Elsevier Inc. All rights reserved.
doi:10.1016/j.bbrc.2011.02.128

Fourteen 5 week old male Sprague Dawley rats (CLEA Japan, Tokyo, Japan) with body weight of 98.7 ± 9.7 g were randomly divided into two groups (transcutaneous CO_2 application group (CO_2) and nontreatment group (Control)). We used 100% CO_2, and transcutaneous CO_2 absorption enhancing hydrogel (CO_2 hydrogel) and a CO_2 adaptor that seals the body surface and retains the gas inside. The ingredients of the CO_2 hydrogel were carbomer (0.65%), glycerin (5.00%), sodium hydroxide (0.18%), sodium alginate (0.15%), sodium dihydrogen phosphate (0.15%), methylparaben (0.10%), and deionized water (balance). The pH of the hydrogel was 5.5 (International patent application number: WO2004/002393). The area of skin covered with the hydrogel was sealed with the adaptor, and CO_2 gas was flowed into the area (Fig. 1).

2.2. Procedure for CO_2 treatment

Under pentobarbital anesthesia (6 ml/kg), we shaved the hair on the lower limbs, and applied the hydrogel. The CO_2 adaptor was attached to the limbs and sealed, and CO_2 was administered into the adaptor for 10 min (Fig. 1). This treatment was performed twice a week for 12 weeks.

2.3. Surgical procedure

After 12 weeks rats were sacrificed and weighed 593.4 ± 30.3 g (CO_2 group) and 617 ± 63.2 g (control group), and the TA muscles of the lower limb were dissected carefully and harvested. The muscle was weighed after excess connective tissue was removed and then immediately frozen in isopentane precooled by liquid nitrogen and stored at −80 °C. Serial 10 μm thick transverse sections were prepared from each block.

2.4. Determination of the relative mitochondrial copy number

Genomic DNA was isolated from a 10 mg transversal slice of midbelly TA using the GenElute Mammalian Genomic DNA Miniprep Kit (SIGMA–ALDRICH, St. Louis, MO, USA). Mitochondrial DNA (mtDNA) content relative to PGC-1α gene was measured using Real-time PCR as described previously [9].

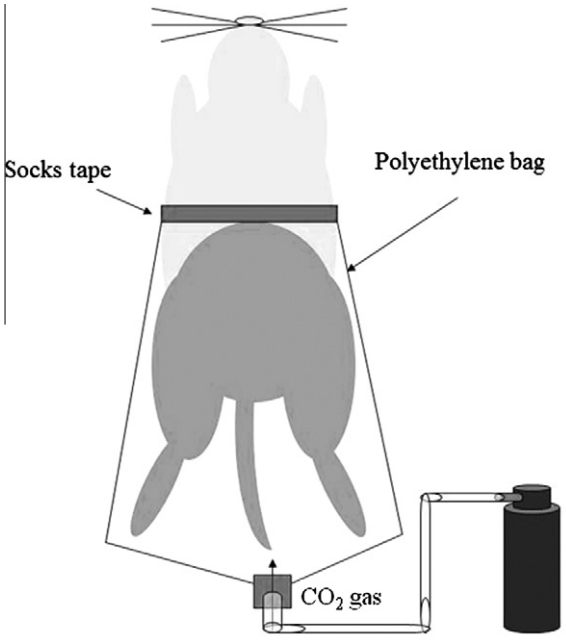

Fig. 1. Shaved lower limbs of rats. Hydrogel was administered, sealed in a polyethylene bag, and CO_2 gas was released into the polyethylene bag twice a week for 3 months.

2.5. Analysis of mRNA expression

2.5.1. Total RNA extraction and reverse transcription

Total RNA was extracted in 500 μl TRIzol reagent (Invitrogen, Carlsbad, CA, USA)/10 mg thinly sliced tissue, and cleaned up by RNeasy Mini Kit (QIAGEN Science, Germantown, MD, USA). Oligo (dT) primed first-strand cDNA was synthesized (50 ng total RNA) using High Capacity cDNA Transcription Kit (Applied Biosystems, FosterCity, CA, USA).

2.5.2. Real-time PCR

Quantification of mRNA transcription (induplicate) was performed in Applied Biosystems StepOne™ Real-Time PCR System (Applied Biosystems, FosterCity, CA, USA). Real-Time PCR reactions (20 μl) contained 0.5 μM forward primer, 0.5 μM reverse primer, and 1 μL of cDNA template from RT reaction, and 10 μl 10 × master mix for Power SYBER green master mix (Applied Biosystems, FosterCity, CA, USA). Reaction conditions included 10 min at 95 °C, followed by 40 cycles at 95 °C (15 s) and 60 °C (1 min). The level of each target gene was normalized to GUSB (β-glucuronidase) levels and expressed relative to the levels of the control group (ΔΔCT methods; Applied Biosystems).

2.5.3. Primers design

All primers used in this study were mRNA specific (on different exons and crossing over to intron) and designed for gene expression Real-time PCR analysis using Primer3 and Primer designing tool (NCBI). Primers for GUSB, the housekeeping gene, were designed to forward (5′-TATCTCTCTCGCAAAATGAAGGC-3′) and reverse (5′-GCTGACTTCATGAC GAACCAG-3′). Primers for PGC-1α were designed to forward (5′-ATGAATGCAGCGGTCTTAGC-3′) and reverse (5′-AACAATGGCAG GGTTTGTTC-3′). Primers for SIRT1 were designed to forward (5′-TCATTCCTGTG AAAGTGATGACGA-3′) and reverse (5′-GCCAATCATGAGGTGTTGCTG-3′). Primers for VEGF-A were designed to forward (5′-GTATATCTTCAAGCCGTCCTGT GTG-3′) and reverse (5′-GATCCG CATGATCTGCATAGTGAC-3′).

Primers for mtDNA were as follows: Forward (5′-ACACCAAAA GGACGA ACCTG-3′) and reverse (5′-ATGGGGAAGAAGCCCTAGAA-3′); for nDNA (β-actin), forward (5′-GCGGTGACCATAGCCCTCTTT-3′) and reverse (5′-TGCCACTCCCAA AGTAAAGGGTCA-3′). All primers were bought from Invitrogen.

2.6. Immunohistochemistry

Skeletal muscle tissue cut into slices along the sagittal plane were pretreated with citrate buffer for 40 min at 95 °C, quenched with 0.05% H_2O_2, and incubated with primary antibody overnight at 4 °C. Rabbit anti-human VEGF polyclonal antibody (Santa Cruz, Delaware Avenue, California, USA), rabbit anti-human PGC-1α polyclonal antibody (Santa Cruz, Delaware Avenue, California, USA), and rabbit anti-human SIRT1 polyclonal antibody (Invitrogen, Carlsbad, CA, USA) were used at a 1:1000 dilution using Can get signal® immunostain (TOYOBO, Osaka, Japan). Following this, sections were incubated with horseradish peroxidase (HRP)-conjugated goat anti-rabbit IgG polyclonal antibody (Nichirei Bioscience, Tokyo, Japan), for 30 min at room temperature. The signal was developed as a brown reaction product using the peroxidase substrate 3, 3-diaminobenzidine (Nichirei Bioscience, Tokyo, Japan). The sections were counterstained with methyl-green for anti-PGC-1α antibody and anti-SIRT1 antibody, and hematoxylin for anti-VEGF antibody.

2.7. ATPase staining

Unfixed frozen TA muscles were sectioned at 10 μm thickness in the cryostat and ATPase staining was performed as previously described with pH 4.6 [10].

2.8. Isolation of myosin heavy chain (MHC)

Protein solution was isolated from a 10 mg transversal slice of midbelly TA using a urea buffer. 5–20 μl of this homogenate were used for MHC analysis using two-dimensional electrophoresis. MHC analysis was as described previously [11]. After electrophoresis, gels were silver-stained using a Wako Silver Stain Kit (Wako Pure Chemical Industries, Ltd., Osaka, Japan). Images of MHC bands were analyzed by LAS-3000, and band intensities were quantified by Scion-Image.

2.9. Statistics analysis

Data are shown as the mean values ± standard deviation. The results of the two groups were analyzed using Mann–Whitney *U* test. The level of statistical significance was set at $P < 0.05$.

3. Results

3.1. TA muscle weight

TA muscle was weighed by an electronic balance (A&D, Japan). Muscle weight ratio was calculated by the following equation: Muscle weight ratio = muscle weight/body weight × 100. The upward tendency of muscle weight and muscle weight ratio in the CO_2 group was observed ($n = 14$). After 3 months in the CO_2 group, the TA muscle weights were 1.112 ± 0.190 g, and the muscle weight ratio was 0.188 ± 0.021. After 3 months in the control group, the TA muscle weights were 1.101 ± 0.128 g, and the muscle weight ratio was 0.178 ± 0.023.

3.2. Real-time PCR analysis

The gene expression of PGC-1α, SIRT1, VEGF-A and the number of mitochondria in the CO_2 group was significantly increased compared to Figs. 2a and b ($n = 12$). The average PGC-1α and VEGF-A in the CO_2 group was more than twice the average of the control group. However, the expression of SIRT1 in the CO_2 group was only 1.4 times of that in control group.

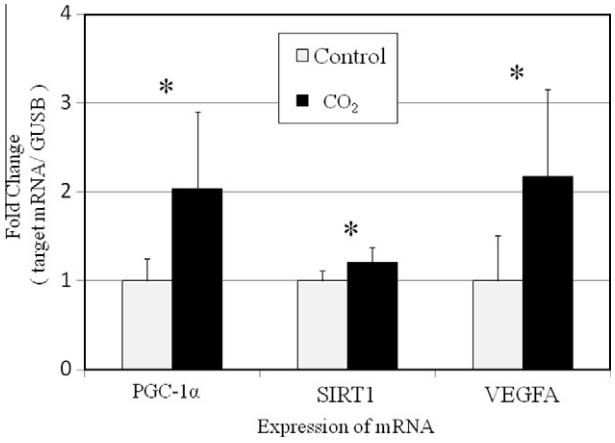

Fig. 2a. Real-time PCR analysis of PGC-1α, SIRT1, and VEGF-A. Control groups are white. CO_2 groups, black. $^*p < 0.05$.

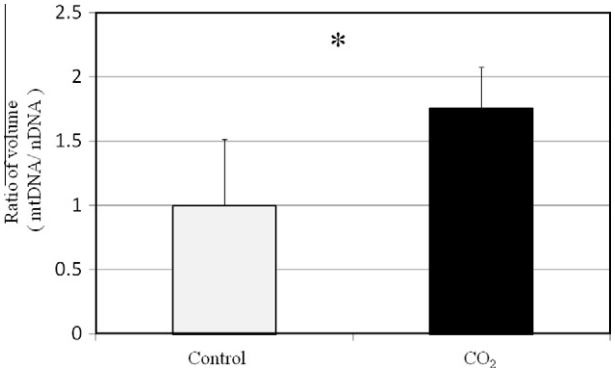

Fig. 2b. Real-time PCR analysis for mitochondrial DNA. Control groups are white. CO_2 groups, black. $^*p < 0.05$.

3.3. Immunohistochemical staining

As shown in Fig. 2c, immunohistochemistry for PGC-1α and SIRT1 revealed that many nuclear were positively stained in the muscle tissue of the CO_2 group. However, there was no positive staining for these proteins in the nuclear in the control group. The results of immunohistochemistry for VEGF showed that the positive staining area in the CO_2 group was much larger, compared

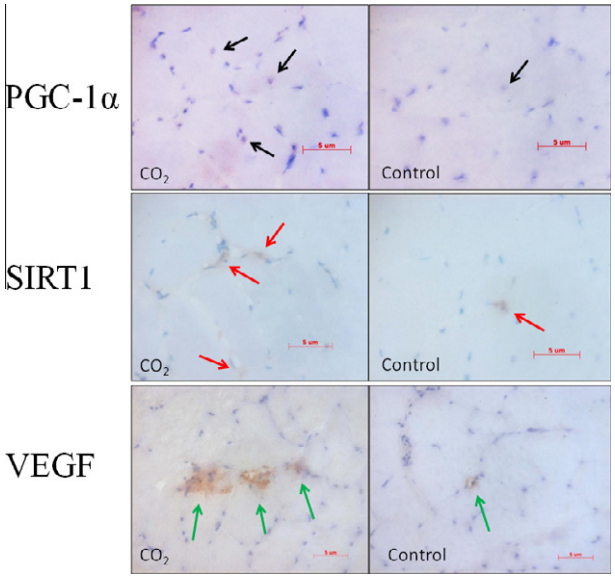

Fig. 2c. Immunohistochemical staining for PGC-1α (black arrow), SIRT1 (red arrow) and VEGF (green arrow) of middle section of TA muscle. (For interpretation of the references in colour in this figure legend, the reader is referred to the web version of this article.)

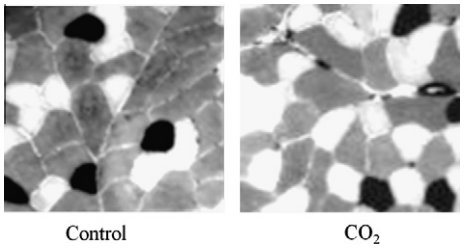

Fig. 3a. ATPase staining (pH 4.6) in the deep layer of TA muscles of the control group and CO_2 group. IIB fibers are gray; IIA fibers, white; I fibers, black.

to the control group. These results were comparable with results of real-time PCR analysis.

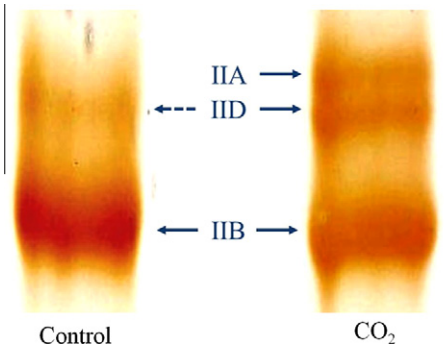

Fig. 3b. Analysis of electrophoresis-based MHC isoform. Control group shows mostly IIB fibers. In contrast, bands of IIB, IIA and IID are observed in the CO_2 group.

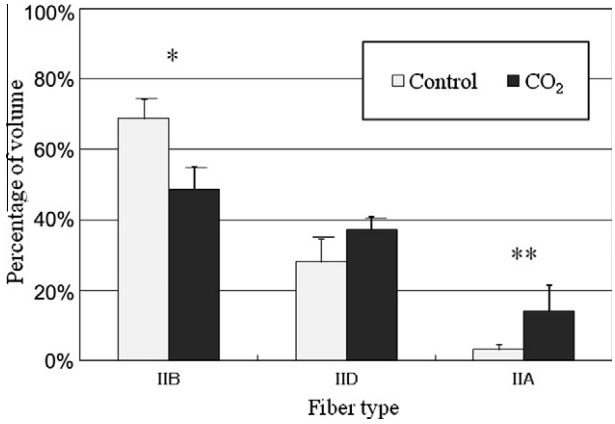

Fig. 3c. Distribution of muscle fiber type. Control groups are white. CO_2 groups, black. $^{*}p < 0.05$, and $^{**}p < 0.01$.

3.4. ATPase staining

Fig. 3a shows the deep layer of TA muscle. IIB fibers are gray, IIA fibers are white, and I fibers are black. In this layer in the CO_2 group, fewer IIB fibers and more IIA fibers were observed in comparison with the control group. I fibers seemed unchanged.

3.5. MHC isoform

As shown in Figs. 3b and c, the percentage of IIB fibers decreased in the CO_2 group, whereas IID fibers and/or IIA fibers increased. A significant difference in the percentage of IIB fibers and IIA fibers between the two groups was observed ($p < 0.05$). In contrast, there was no significant difference in the percentage of IID fibers between the two groups ($n = 12$). The changes in the CO_2 group are similar to those observed after exercise [12].

4. Discussion

Skeletal muscle is the largest organ in the human body, comprising about 40% of body weight. The mass and composition of skeletal muscle are critical for functions, such as exercise, energy expenditure, and glucose metabolism [13,14]. Elderly humans are known to undergo a progressive loss of muscle fiber associated with diabetes, obesity, and decreased physical activity [15]. In human skeletal muscle, there are two major classifications of fiber type: Type I (slow-twitch oxidative, or so-called red muscle) and type II (fast-twitch glycolytic, or so-called white muscle) fibers. Mass, fiber size, and fiber composition in adult skeletal muscle are regulated in response to changes in physical activity, environment, or pathological conditions. Moreover Type II can be classified as IIA, IID, and IIB. These fibers have individually different characteristics of production of ATP, the number of mitochondria, and capillary density. IIA and IID fibers have a higher percentage of these substances than IIB [16,17]. Specifically, endurance exercise training leads to fiber type transformation from IIB to IID and IIA, mitochondrial biogenesis, angiogenesis, and other adaptive

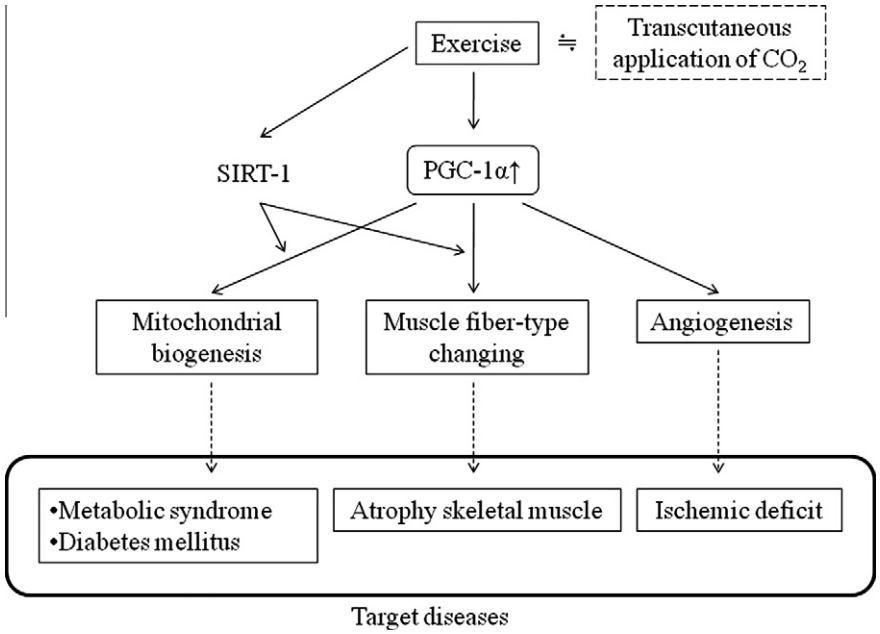

Fig. 4. Aerobic exercise generally induces an increase of PGC-1α, mitochondrial biogenesis, muscle fiber-type changing, and angiogenesis, because of increasing aerobic metabolism as a result of an increase in pO_2 in vasodilatation and the Bohr effect. Our findings indicated that transcutaneous application of CO_2 could cause a similar effect on muscle to aerobic exercise, suggesting that the transcutaneous application of CO_2 may have a therapeutic potential for muscular strength recovery resulting from disuse atrophy in post-operative patients and the elderly population.

changes in skeletal muscle along with improved insulin sensitivity and metabolic flexibility in both rodents and humans [18]. The orchestrated regulation of these processes is of extreme elegance, and it is reported that PGC-1α is key player for several of these adaptations [19,20].

Generally, PGC-1α is induced by exercise and mediates known responses to exercise, such as mitochondrial biogenesis, muscle fiber-type switching, up-regulation of VEGF and neovascularization [21]. This links the regulation of consumption of oxygen by mitochondria to the delivery of oxygen and nutrients by the vasculature. In addition, SIRT1 also supports mitochondrial biogenesis and the muscle fiber-type changing pathway [18–24].

In the current study, we demonstrated that transcutaneous application of CO_2 up-regulated the gene expression of PGC-1α, SIRT1 and VEGF, and increased the numbers of mitochondria. These changes were similar to those observed as a result of aerobic exercise.

One possible mechanism for the up-regulation of VEGF in TA muscle by transcutaneous application of CO_2 is that a low intracellular pH in muscle induced by CO_2 trascutaneous application could trigger the transcriptional activation of VEGF. Xu et al. reported the transcriptional activation of the VEGF gene by low pH in human glioblastoma cells [25]. In our previous study, we demonstrated using ^{31}P-MRS that transcutaneous application of CO_2 significantly lowered the intracellular pH of treated muscle [7].

Transcutaneous application of CO_2 also promoted TA muscle fiber switching. Usually muscle fibers transform from IIB fibers to IID fibers and IIA fibers as a result of exercise, whereas in the long-term bed rest situation they transform from IIA to IIB fibers. Our result clearly showed that TA muscle fibers in which CO_2 was transcutaneously applied transformed from IIB fibers to IID fibers and/or IIA fibers. That is to say, transcutaneous application of CO_2 induced similar changes to exercise in TA muscle.

Aerobic exercise induces an increase of PGC-1α, and mitochondrial biogenesis, muscle fiber-type switching, and angiogenesis, because of increasing aerobic metabolism as a result of an increase in O_2 pressure in vasodilatation and the Bohr effect. Previously our study suggested that transcutaneous application of CO_2 leads to an increase of the O_2 pressure in treated tissue, thus potentially causing an "artificial Bohr effect". Our findings indicated that transcutaneous application of CO_2 could cause a similar effect on muscle to aerobic exercise (Fig. 4). The current study also suggests that the transcutaneous application of CO_2 may have a therapeutic potential for muscular strength recovery resulting from disuse atrophy in post-operative patients and the elderly population.

Acknowledgments

The authors wish to express sincere thanks to Ms. Kyoko Tanaka, Ms. Maya Yasuda, and Ms. Minako Nagata (Department of Orthopaedic Surgery, Kobe University Graduate School of Medicine) for their technical assistance; and Prof. Masanobu Wada (Graduate School of Integrated Arts and Sciences, Hiroshima University) for excellent technical assistance in ATPase staining and silver staining; and Janina Tubby for English rewriting.

References

[1] M. Goodman, G.W. Moore, G. Matsuda, Darwinian evolution in the genealogy of haemoglobin, Nature 253 (1975) 603–608.
[2] R.M. Wells, Evolution of heamoglobin function: molecular adaptations to environment, Clin. Exp. Pharmacol. Physiol. 26 (1999) 591–595.
[3] C. Bohr, K. Hasselbach, A. Krogh, Ueber emen in biologischen Bezuehung wichtigen Einfluss, den die Kohlen saurespannung des Blutes anf dessen Samerstoffbinding ubt, Arch. Physiol. 16 (1904) 402.
[4] A. Riggs, The nature and significance of the bohr effect in mammalian hemoglobins, J. Gen. Physiol. 43 (1960) 737–752.
[5] I. Tyuma, The Bohr effect and the Haldane effect in human hemoglobin, Jpn. J. Physiol. 34 (1984) 205–216.
[6] F.B. Jensen, Red blood cell pH, the Bohr effect, and other oxygenation-linked phenomena in blood O_2 and CO_2 transport, Acta Physiol. Scand. 182 (2004) 215–227.
[7] Y. Sakai, M. Miwa, K. Oe, T. Niikura, S.Y. Lee, A. Koh, T. Iwakura, M. Kurosaka, The evidence for the Bohr effect in the human body using a novel system for transcutaneous application of CO_2, Trans. Ortop. Res. Soc. 57 (2011) 393.
[8] M. Iwabu, T. Yamauchi, M. Okada-Iwabu, K. Sato, T. Nakagawa, M. Funata, M. Yamaguchi, S. Namiki, R. Nakayama, M. Tabata, H. Ogata, N. Kubota, I. Takamoto, Y.K. Hayashi, N. Yamauchi, H. Waki, M. Fukuyama, I. Nishino, K. Tokuyama, K. Ueki, Y. Oike, S. Ishii, K. Hirose, T. Shimizu, K. Touhara, T. Kadowaki, Adiponectin and AdipoR1 regulate PGC-1 alpha and mitochondria by Ca(2+) and AMPK/SIRT1, Nature 464 (2010) 1313–1319.
[9] N.M. van den Broek, J. Ciapaite, H.M. De Feyter, S.M. Houten, R.J. Wanders, J.A. Jeneson, K. Nicolay, J.J. Promper, Increased mitochondrial content recues in vivo muscle oxidative capacity in long-term high-fat-diet-fed rats, FASEB J. 24 (2010) 1354–1364.
[10] M.H. Brooke, K.K. Kaiser, Muscle fiber types: how many and what kind?, Arch Neurol. 23 (1970) 369–379.
[11] A. Saitoh, T. Okumoto, H. Nakano, M. Wada, S. Katsuta, Age effect on expression of myosin heavy and light chain isoforms in suspended rat soleus muscle, J. Appl. Physiol. 86 (1999) 1483–1489.
[12] M. Wada, S. Inashima, T. Yamada, S. Matsunaga, Endurance training-induced changes in alkali light chain patterns in type IIB fibers of the rat, J. Appl. Physiol. 94 (2002) 923–929.
[13] F. Zurlo, K. Larson, C. Bogardus, E. Ravussin, Skeletal muscle metabolism is major determinant of resulting energy expenditure, J. Clin. Investig. 86 (1990) 1423–1427.
[14] M.W. Berchtold, H. Brinkmeier, M. Muntener, Calcium ion in skeletal muscle: its crucial role for muscle function, plasticity, and disease, Physiol. Rev. 80 (2000) 1215–1265.
[15] D.N. Proctor, P. Balagopal, K.S. Nair, Age-related sarcopenia in humans is associated with reduced synthetic rates of specific muscle proteins, J. Nutr. 128 (1998) 351–355.
[16] S. Ennion, J. Sant'ana Pereira, A.J. Sargeant, A. Young, G. Goldspink, Characterization of human skeletal muscle fibres according to the myosin heavy chains they express, J. Muscle. Res. Cell. Motil. 16 (1995) 35–43.
[17] A. Termin, R.S. Staron, D. Pette, Myosin heavy chain isoforms in histochemically defined fiber types of rat muscle, Histochemistry 92 (1989) 453–457.
[18] V.A. Lira, C.R. Benton, Z. Yan, A. Bonen, PGC-1 alpha regulation by exercise training and its influences on muscle function and insulin sensitivity, Am. J. Physiol. Endocrinol. Metab. 299 (2010) 145–161.
[19] Z. Wu, P. Puigserver, U. Andersson, C. Zhang, G. Adelmant, V. Mootha, A. Troy, S. Cinti, B. Lowell, R.C. Scarpulla, B.M. Spiegelman, Mechanism controlling mitochondrial biogenesis and respiration through the thermogenic coactivator PGC-1, Cell 98 (1999) 115–124.
[20] J. Lin, H. Wu, P.T. Tarr, C.Y. Zhang, Z. Wu, O. Boss, L.F. Michael, P. Puigserver, E. Isotani, E.N. Olson, B.B. Lowell, R. Bassel-Duby, B.M. Spiegelman, Transcriptional co-activator PGC-1 alpha drives the formation of slow-twitch muscle fibres, Nature 418 (2002) 797–801.
[21] Z. Arany, S.Y. Foo, Y. Ma, J.L. Ruas, A. Bommi-Reddy, G. Girnun, M. Cooper, D. Laznik, J. Chinsomboon, S.M. Rangwala, K.H. Baek, A. Rosenzweig, B.M. Spiegelman, HIF-independent regulation of VEGF and angiogenesis by the transcriptional coactivator PGC-1alpha, Nature 451 (2008) 1008–1012.
[22] S.P. Naples, S.J. Borengasser, R.S. Rector, G.M. Uptergrove, E.M. Mikus, L.G. Koch, S.L. Britton, J.A. Ibdah, J.P. Thyfault, Skeletal muscle mitochondrial and metabolic responses to a high-fat diet in female rats bred for high and low aerobic capacity, Appl. Physiol. Nutr. Metab. 35 (2010) 151–162.
[23] Y. Kamei, S. Miura, M. Suzuki, Y. Kai, J. Taniguchi, K. Mochida, T. Hata, J. Matsuda, H. Aburatani, I. Nishino, O. Ezaki, Skeletal muscle FOXO1 (FKHR) transgenic mice have less skeletal muscle mass, down-regulated Type I (slow twitch/red muscle) fiber genes, and impaired glycemic control, J. Biol. Chem. 279 (2004) 41114–41123.
[24] H. Irie, T. Tatsumi, M. Takamiya, K. Zen, T. Takahara, A. Azuma, K. Tateishi, T. Nomura, H. Hayashi, N. Nakajima, M. Okigaki, Carbon dioxide-rich water bathing enhances collateral blood flow in ischemic hindlimb via mobilization of endothelial progenitor cells and activation of NO-cGMP system, Circulation 111 (2005) 1523–1529.
[25] L. Xu, D. Fukumura, R.K. Jain, Acidic extracellular pH induces vascular endothelial growth factor (VEGF) in human glioblastoma cells via ERK1/2 MAPK signaling pathway: mechanism of low pH-induced VEGF, J. Biol. Chem. 277 (2002) 11368–11374.